

**Electronic Supplementary Information:**  
**Wide-angle X-ray scattering and molecular  
dynamics simulations of supercooled protein  
hydration water**

Maddalena Bin,<sup>†</sup> Rafat Yousif,<sup>†</sup> Sharon Berkowicz,<sup>†</sup> Sudipta Das,<sup>†</sup> Daniel  
Schlesinger,<sup>‡</sup> and Fivos Perakis<sup>\*,†</sup>

*<sup>†</sup>Department of Physics, AlbaNova University Center, Stockholm University, 106 91  
Stockholm, Sweden*

*<sup>‡</sup>Department of Environmental Science & Bolin Centre for Climate Research, Stockholm  
University, 106 91 Stockholm, Sweden*

E-mail: [f.perakis@fysik.su.se](mailto:f.perakis@fysik.su.se)

# Contents

<b>1</b>	<b>Experimental methods and results</b>	<b>S3</b>
1.1	Hydration level estimates by thermo-gravimetric analysis . . . . .	S3
1.2	Scattering intensity with hydration level $h = 0.47$ . . . . .	S3
1.3	Sample preparation . . . . .	S5
1.4	X-ray scattering setup and measurement protocol . . . . .	S5
1.5	Peak position of hydrated lysozyme powder . . . . .	S8
<b>2</b>	<b>Simulation methods</b>	<b>S9</b>
2.1	MD simulation equilibration . . . . .	S9
2.2	Scattering intensity calculations . . . . .	S9
	<b>References</b>	<b>S11</b>

# 1 Experimental methods and results

## 1.1 Hydration level estimates by thermo-gravimetric analysis

The lysozyme protein powders with hydration level  $h = 0.05$  were measured without any drying process. Therefore, the amount of residual residual water still present in the protein powder was estimated to  $h = 0.05$  by use of thermo-gravimetric analysis (TGA), shown in Fig. S1 where the weight loss is plotted as a function of the temperature. The hydration water fully evaporates at 400 K. The weight decrease above 500 K is caused by evaporation of the protein components in the form of nitrogen and oxygen gas.

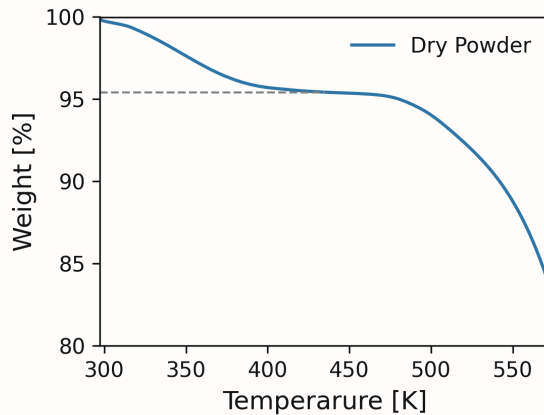


Figure S1: Weight loss of dry protein powder in % measured as a function of temperature by means of thermo-gravimetric analysis. The residual hydration water evaporates until 400 K and is estimated to be the 5% of the total mass. The weight decrease above 500 K is caused by evaporation of the protein components in the form of nitrogen and oxygen gas.

## 1.2 Scattering intensity with hydration level $h = 0.47$

Fig. S2 shows the experimental scattering intensity as a function of the momentum transfer  $Q$  for the hydration level  $h = 0.47$ . Here, the temperature ranges from  $T = 290$  K to  $T = 235$  K (colored lines). For higher temperatures, the shoulder of the peak at  $Q = 1.54 \text{ \AA}^{-1}$  is more pronounced compared to the lower hydration, which is consistent with the larger amount of water molecules present in the sample. Between 245 and 235 K, the sample crystallizes

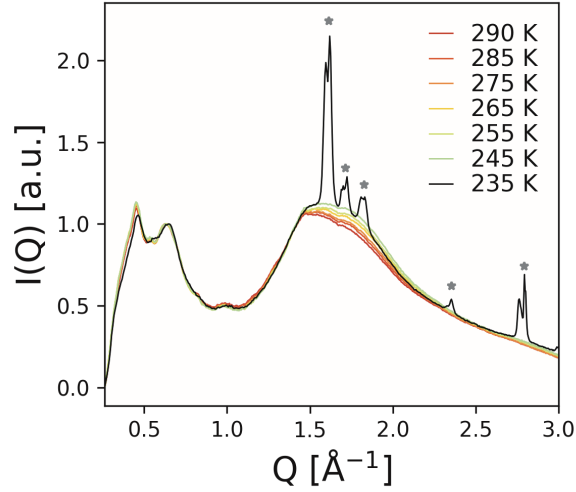


Figure S2: The hydration water scattering intensity as a function of the momentum transfer obtained experimentally at variable temperatures for hydration  $h = 0.47$ . Freezing is evident by the presence of Bragg peaks, indicated by the asterisks.

(black solid line), which is evident from the characteristic Bragg peaks of ice  $Ih^1$  indicated by the asterisks. Before crystallization, the sample exhibits similar features with that at lower hydration level, such as the decreasing intensity of the peak at  $Q = 0.65 \text{ \AA}^{-1}$ , the shift of the peak at  $Q = 1.54 \text{ \AA}^{-1}$  towards higher momentum transfer as well as the enhancement of the shoulder at  $Q \approx 1.7 \text{ \AA}^{-1}$  upon cooling.

### 1.3 Sample preparation

A custom setup was used for preparing the hydrated protein powders which allowed control of the humidity level inside the chamber. Nitrogen gas with a pressure of  $\approx 1.5$  bar was connected to a glass bottle filled with Milli-Q water, which was heated up by a Peltier element at a temperature of  $T \approx 340$  K. Due to the nitrogen pressure, the water vapor was directed by a tube into a closed chamber containing the protein powder. The chamber was connected to a thermal shaker, which allowed to control the temperature of the chamber. A quantity of 200 mg of the lysozyme powder with  $h = 0.05$  was spread onto a small dish and placed in the humidity chamber, which was then cooled at  $T = 278$  K and exposed to water vapor. The humidity level inside the chamber was controlled by the concurrence of different parameters, such as the nitrogen gas pressure, the vapor and sample temperature. These conditions allowed to get on average 70% of relative humidity, measured with a humidity sensor in the chamber. The sample exposure time to water vapor under these conditions was varied between between 1 and 1.5 hours, corresponding to hydration values  $h = 0.25$  to  $h = 0.47$ .

The  $h$  value was determined by weighing the sample before and after the hydration process multiple times, utilizing a scale with sensitivity  $10^{-3}$  g, where the hydration level is defined as  $h = m_{water}/m_{protein}$ . The hydration value was then determined by estimating the ratio  $h = (m_f - m_i)/(m_i - m_d)$ , where  $m_i$  and  $m_f$  is the mass of the protein powder on the corresponding sample container before and after the hydration process respectively, and  $m_d$  is the mass of the sample container.

### 1.4 X-ray scattering setup and measurement protocol

A D8-Venture manufactured by Bruker Corporation X-ray diffractometer was used, utilising a Copper  $K\alpha$  radiation source with a wavelength of  $\lambda=1.54$  Å and energy  $E = 8041$  eV. The sample was measured in transmission geometry using Shutterless PHOTON 100 CMOS detector, with  $1024 \times 1024$  pixels of  $96 \mu\text{m}$  edge. The cooling system used (Oxford Cryosystems 700

Series Cryostream Cooler) utilises a nitrogen flow and allows us to measure at temperatures ranging from 175 to 290 K.

At the beginning of each measurement, silver behenate was first measured as a calibrator, as its diffraction pattern features several rings in the given momentum transfer range. The beam center was estimated by fitting the Silver behenate rings, as shown in Fig. S3 (left panel). Subsequently, the angular integration of the scattering intensity was performed and the results are shown in Fig.S3 (right panel) where the vertical dashed lines represent the reference values of the Bragg peaks.<sup>2</sup> The calibrator was followed by the background measurements, including the empty Kapton capillary and air contributions. Subsequently, the room temperature measurements were done, screening samples with different  $h$  values. The selected samples were measured at a broad temperature range, starting from  $T = 290$  K to  $T = 175$  K temperatures with steps of 10 K. The ramp rate was set at 360 K/hour and after each temperature was reached we waited five minutes in order to ensure thermal equilibrium based on the X-ray scattering patterns. In order to estimate a potential temperature offset between the measured and actual temperature, tests were performed by measuring the melting point of pure water, which indicate a systematic offset of +5 K, which was corrected in the data.

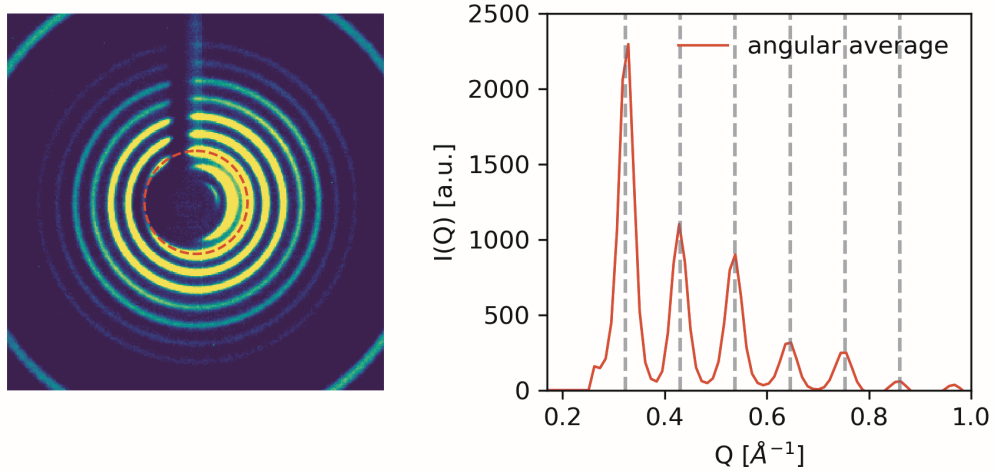


Figure S3: Silver behenate used for  $Q$ -calibration. Left panel: scattering pattern of Silver behenate, for which the first ring was fitted in order to estimate the beam center. Right panel: angularly integrated scattering intensity of Silver behenate shown with the reference values (gray dashed lines).

## 1.5 Peak position of hydrated lysozyme powder

Fig. S4 shows the position of peak iii, as labeled in Fig. 2A, as a function of temperature for the hydrated lysozyme powder with  $h = 0.25$  (blue squares) and  $h = 0.05$  (red circles). The curves were fitted with a Gaussian function in the  $Q$  range  $1.37, 1.56 \text{ \AA}^{-1}$ , from which the peak position was extracted.

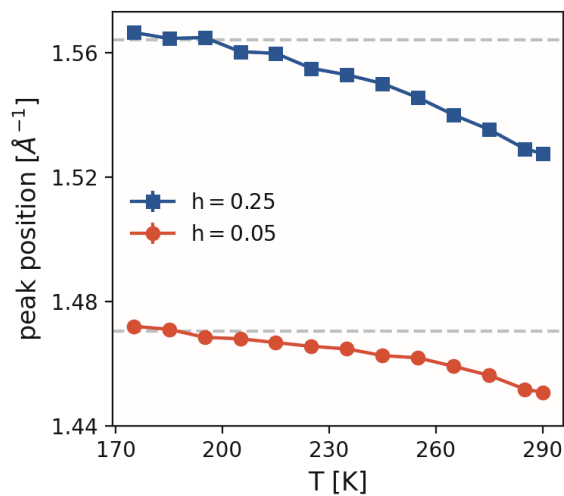


Figure S4: The experimentally extracted position of peak iii as a function of temperature for  $h = 0.25$  (blue squares) and  $h = 0.05$  (red circles).

## 2 Simulation methods

### 2.1 MD simulation equilibration

The density of the system during NPT equilibration (as discussed in the main manuscript) for both bulk TIP4P-EW and hydrated protein powder ( $h = 0.23$ ) is shown for the lowest temperatures,  $T = 230 - 180$  K, in Fig. S5 and S6 respectively. At the lowest temperatures simulated, we note that the total drift of the reported density values for bulk TIP4P-EW is less than  $0.3 \text{ kg/m}^3$  for the last 100 ns of the NPT equilibration.

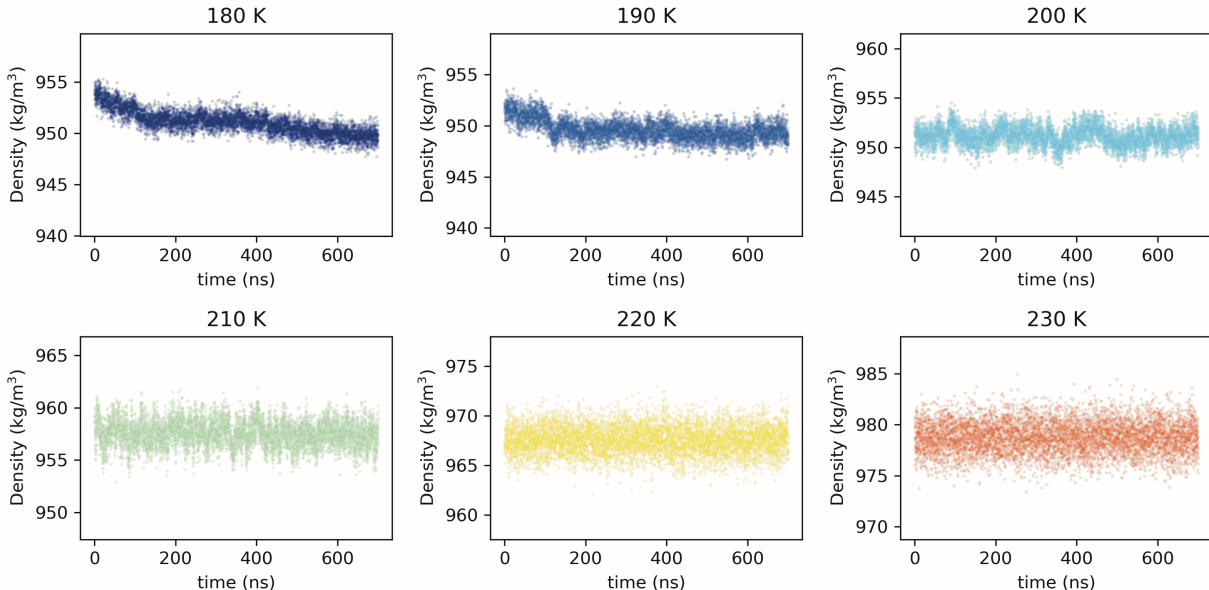


Figure S5: The density of simulated bulk water (TIP4P-EW) during NPT equilibration.

### 2.2 Scattering intensity calculations

The X-ray scattering intensity calculation is based on previous approaches.<sup>3,4</sup> The scattering intensity originating from atom  $i$  and  $j$  is calculated by:

$$I(Q) = \sum_i \sum_j f_i(Q) f_j(Q) e^{-iQ(r_i - r_j)} \quad (1)$$

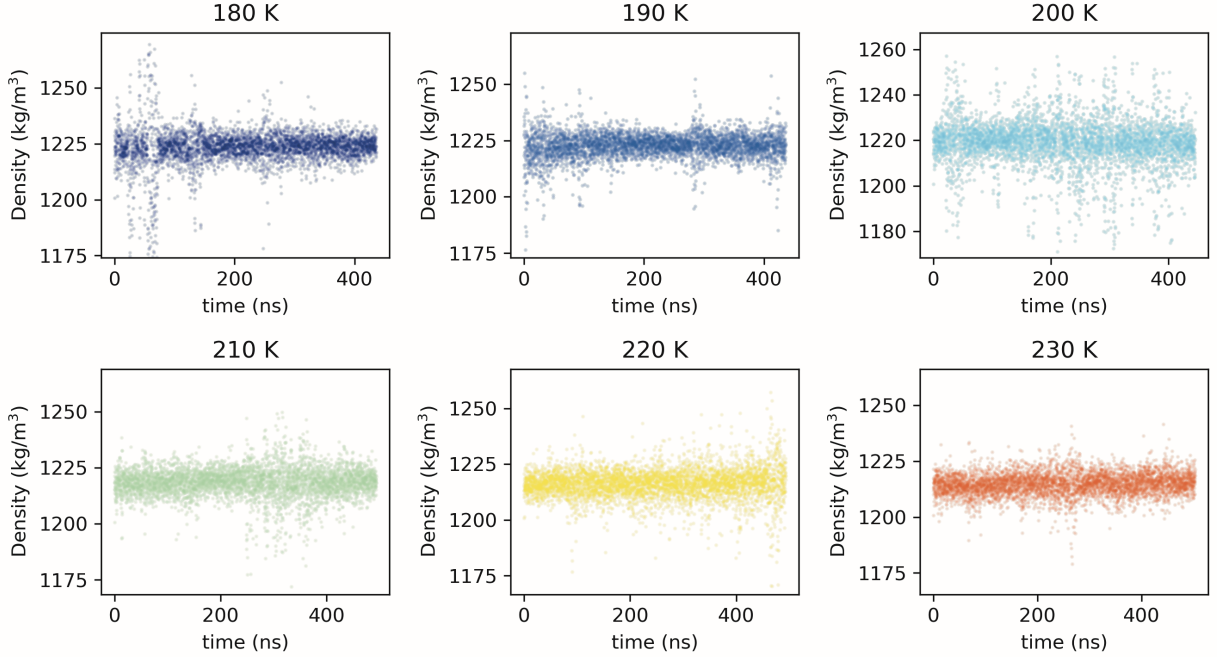


Figure S6: The density of the hydrated protein system  $h = 0.23$  during NPT equilibration.

where  $r_i - r_j$  is the distance between  $i$  and  $j$  and the corresponding atomic form factors  $f_i(Q)$  and  $f_j(Q)$  were calculated based on Cromer-Mann method,<sup>5</sup> by:

$$f_j(Q) = \sum_i a_j e^{-b_j(Q/4\pi)} + c \quad (2)$$

where the  $a_j$ ,  $b_j$  and  $c$  coefficients of the analytical approximation to the atomic form factor were taken from tabulated values obtained with the Hartree-Fock model.<sup>5</sup> Spherical averaging was performed by using the spiral method.<sup>3,4</sup> A set of  $N$  points equally spaced along a Fibonacci spiral on the unit sphere was defined by

$$\theta_j = \arccos(1 - 2j/N), \quad \phi_j = \pi(1 + \sqrt{5})j \quad (3)$$

for  $j = 1, 2, \dots, N$ . The spherical averaging is calculated by averaging over the solid angles defined by the spherical coordinates. With  $N = 100$ , which we find that with the number of proteins in the system is sufficient to produce accurate spherical quadrature.

## References

- (1) Dowell, L. G.; Rinfret, A. P. Low-Temperature Forms of Ice as Studied by X-Ray Diffraction. *Nature* **1960**, *188*, 1144–1148.
- (2) Huang, T. C.; Toraya, H.; Blanton, T. N.; Wu, Y. X-ray powder diffraction analysis of silver behenate, a possible low-angle diffraction standard. *J. Appl. Crystallogr.* **1993**, *26*, 180–184.
- (3) Nguyen, H. T.; Pabit, S. A.; Meisburger, S. P.; Pollack, L.; Case, D. A. Accurate small and wide angle x-ray scattering profiles from atomic models of proteins and nucleic acids. *J. Chem. Phys.* **2014**, *141*, 22D508.
- (4) Park, S.; Bardhan, J. P.; Roux, B.; Makowski, L. Simulated x-ray scattering of protein solutions using explicit-solvent models. *J. Chem. Phys.* **2009**, *130*, 134114.
- (5) Cromer, D. T.; Mann, J. B. X-ray scattering factors computed from numerical Hartree–Fock wave functions. *Acta Crystallogr. A* **1968**, *24*, 321–324.